

Expert-Token Resonance: Redefining MoE Routing through Affinity-Driven Active Selection

Jing Li*, Zhijie Sun*, Dachao Lin*, Qiqian Fu*, Xuan He, Binfan Zheng, Yi Lin, Li Zeng,
Rongqian Zhao, Xin Chen
Huawei Technologies Co., Ltd

Abstract

Mixture-of-Experts (MoE) architectures have emerged as a paradigm-shifting approach for large language models (LLMs), offering unprecedented computational efficiency. However, these architectures grapple with challenges of token distribution imbalance and expert homogenization, impeding optimal semantic generalization. We introduce a novel framework that redefines MoE routing through affinity-driven active selection. The innovations for the framework encompass: (1) A rigorous formulation of expert-token affinity metrics. (2) An adaptive bidirectional selection mechanism leveraging resonance between experts and tokens. (3) Theoretical derivation and experimental evidence of reduced expert capacity bounds under dynamic token distribution evolution. It is also integrated with orthogonal feature extraction module and an optimized loss function for expert localization. Our theoretical analysis demonstrates that this approach mitigates expert homogenization while enabling substantial capacity boundary reduction. Experimental validation corroborates these findings: it achieves a 40% reduction in token processed by each expert without compromising model convergence or efficacy. When coupled with communication optimizations, the training efficiency improvements of 5.4% to 46.6% can be observed. After supervised fine-tuning, it exhibits performance gains of 9.7% to 14.1% across GDAD, C-Eval, and TeleQnA benchmarks.

Introduction

Large language models (LLMs) have shown exceptional proficiency in understanding deep structures and complex semantic relationships within language (Zhao et al. 2023). As these models scale up, their capabilities in language generation and logical comprehension are enhanced, but this comes at the cost of significant computational, communication, and storage demands (Jiang et al. 2024b). To scale models efficiently without disproportionately increasing computational costs, researchers have incorporated the Mixture-of-Experts (MoE) architecture into LLMs (Lepikhin et al. 2020). The MoE framework integrates multiple experts within the model, each tasked with processing specific types of inputs (Fedus, Zoph, and Shazeer 2022). For a given input, only a subset of experts is activated, allowing for more efficient use of computational resources (Du et al.

2022). Recently, several LLMs employing MoE structures, such as DeepSeek-MoE (Dai et al. 2024) and Mixtral (Jiang et al. 2024a), have demonstrated outstanding performance on various leaderboards.

Despite the efficiency benefits of MoE in scaling model sizes, it introduces several new challenges and drawbacks (Shazeer et al. 2017). The conventional MoE model’s convergence and the experts’ generalization capabilities are heavily dependent on the design of the routing strategy, which easily leads to an imbalanced “winner-takes-all” phenomenon among experts. The imbalance between excessively “developed” experts and those lacking adequate training may compromise or even nullify the intended functionality of routing strategies. Recent studies address these challenges from multiple perspectives (Li et al. 2023). DeepSeek-MoE (Dai et al. 2024) introduces the concept of the vertical-class expert, which is created through fine-grained partitioning, and the shared experts are always activated. This approach minimizes the constraints on expert specialization imposed by knowledge hybridity and knowledge redundancy. StableMoE (Dai et al. 2022) proposes a two-stage training approach to address the issue of routing fluctuation. This method involves training the routing network independently from the backbone model and utilizing a frozen, distilled routing mechanism to allocate tokens. The characteristics of classical gated routing lead to experts being unable to learn features mastered by other experts. To address this, MoDE (Xie et al. 2024) proposes moderate distillation between experts to mitigate the generalization problems caused by narrow learning paths. DYNMoE (Guo et al. 2024) introduces a unique gated routing mechanism capable of adaptively determining the number of activated experts through trainable expert thresholds, even allowing for the addition or removal of experts.

In addition to the classical token choice scenario, previous researches also propose work utilizing expert choice (EC). Google Brain introduces the EC routing algorithm (Zhou et al. 2022), which assigns experts with predetermined buffer capacities to the Top-k tokens to ensure load balance. The Brainformer (Zhou et al. 2023) also adopts this routing strategy, constructing a trainable gating matrix to project the input feature space onto scores corresponding to each expert. Then, each token is routed to the Top-k experts. This strategy is proven highly effective in achieving expert

*These authors contributed equally.

load balancing and enhancing expert learning outcomes.

The design of routing strategy is crucial to the MoE structure, while not all tokens may be suitable for training (Riquelme et al. 2021). In addition to data preprocessing techniques such as dataset cleaning and deduplication, previous studies have also considered how to discard certain tokens within the model. Early work introduced the concept of expert capacity (Lepikhin et al.), which refers to the maximum number of tokens each expert can process at once. Tokens exceeding this capacity are discarded. Expert capacity helps to ensure load balance among experts while facilitating All-to-All communication implementation. However, in situations where it is uncertain whether a token contributes to training, there is a risk of discarding class-discriminative samples, potentially compromising the model’s training outcomes. XMoE (Yang et al. 2024) achieves more precise router by implementing a threshold-based approach. If a token reaches the specified threshold, it is processed exclusively by a single expert while being discarded by other experts within the Top-k selection. This method allows for more nuanced token selection and processing. LocMoE (Li et al. 2024) leverages orthogonal routing weights to prevent token homogenization across different expert networks and introduces the Grouped Average Pooling (GrAP) layer (Wang, Zhang, and Du 2023) for token feature extraction. Under these conditions, LocMoE also provides the theoretical proof for the lower bound of expert capacity.

In this paper, we propose expert-token resonance, a mechanism consisting of an expert-token bidirectional selection router and the adaptive expert capacity strategy. The primary contributions of this paper are as follows:

1. **A rigorous formulation of expert-token affinity metrics.** Given that expert selection is related to the angle between tokens and gating weights, the cosine similarity between tokens and gating weights is used to define the affinity score between tokens and experts. We provide theoretical analysis of utilizing the affinity score for better guiding expert choice routers to focus on different segmentations of tokens, thus mitigating the homogenization tendency. Further, we incorporate affinity scores into the design of our bidirectional selection router.
2. **Expert-token bidirectional selection.** By integrating the concepts of expert choice router (ECR) and token choice router (TCR), we propose the adaptive bidirectional selection mechanism. Contrast to conventional router, the bidirectional selection router allows MoE to enhance the training success rate while considering expert capacity constraints. Its effectiveness has been theoretically validated.
3. **The adaptive expert capacity bound.** Setting an adaptive affinity threshold allows the lower bound of expert capacity to be significantly reduced. As training iterations increase, the information density of token features grows, causing the expert capacity to initially decrease and then stabilize. Ultimately, the training efficiency of MoE can be greatly enhanced.

Expert-token resonance mechanism adopts the state-of-the-art MoE model Mixtral $8\times 7B$ as the backbone, and uti-

lizes AscendSpeed and ModelLink libraries for pre-training on Ascend NPU clusters. Experiments conducted on clusters with 32, 64, and 256 NPUs indicate that our approach improves training efficiency by 5.4% to 46.6% compared to the baseline, and by 2.9% to 13.3% compared to LocMoE. Model performance is enhanced by 9.7% to 14.1% compared to the baseline, and by 1.7% to 4.1% compared to LocMoE.

The rest of this paper is structured as follows: Section **Related Work** introduces related work on LLMs, MoE, and the Ascend architecture. Section **Method** reviews LocMoE and presents the methods proposed in this paper, along with theoretical evidence. Section **Experiments** analyzes the experimental results of our approach regarding training efficiency and model performance. The final section summarizes the content of this paper and offers an outlook on future improvements.

Related Work

LLMs. BERT (Kenton and Toutanova 2019) and GPT (Radford et al.) in 2018 marked the emergence of the LLM era. GPT-3 (Floridi and Chiriatti 2020), with 175 billion parameters, demonstrated impressive capabilities in language understanding and generation in 2020. By 2023-2024, LLMs expanded to hundreds of billions to trillions of parameters: GPT-4 (Achiam et al. 2023) achieved breakthroughs in zero-shot and few-shot learning; PaLM-2 (Anil et al. 2023) enhanced knowledge acquisition and reasoning; Chinchilla (Hoffmann et al. 2022) optimized computational resources and model scale; and Claude-v1 (Wei, Haghtalab, and Steinhardt 2024) displayed a safer, human-aligned LLM. These LLMs have made significant advancements across domains, paving the way towards artificial general intelligence.

MoE. Despite the outstanding performance of LLMs in language understanding and generation, their high computational cost hinders further model scale expansion. To alleviate this issue, researchers have introduced the MoE architecture, which incorporates multiple expert modules and dynamically selects a subset of experts to process inputs, significantly reducing computational overhead while maintaining performance. GShard (Lepikhin et al. 2020) and Switch Transformer (Fedus, Zoph, and Shazeer 2022) employ Top-2 and Top-1 routing strategies, respectively, to mitigate the expert load imbalance problem. Hash Layer (Roller et al. 2021) adopt hashing techniques to simplify the gating mechanism and improve model performance. METRO (Bajaj et al. 2022) introduces a metric learning-based routing mechanism that guides expert selection by learning task-relevant metric functions, enhancing the model’s generalization ability. DSelect-k (Hazimeh et al. 2021) proposes a dynamic selection algorithm based on Markov chains, adaptively choosing the number of experts to maintain performance while reducing training costs. Furthermore, DeepSpeed-MoE (Rajbhandari et al. 2022) optimizes expert parallelism and pipeline parallelism in MoE, further boosting training efficiency. These works lay the foundation for the subsequent application of MoE in LLMs.

Ascend Architecture. The AI Core in the Ascend 910B NPU adopts the DaVinci architecture (Tang and Wang 2023), which is responsible for executing computation-intensive operators related to scalars, vectors, and 3D cubes, and is widely used in LLM training. Huawei’s proprietary cache coherence protocol interconnect, High Confidence Computing Systems (HCCS) (Xia et al. 2021), enables high-performance inter-device data communication in multi-card scenarios. The Huawei Collective Communication Library (HCCL) (Cao et al. 2024), designed for the Ascend processor, offers high-performance primitives for single-node multi-card and multi-node multi-card collective communication. It implements collective communication functions on PCIe, HCCS, and RoCE high-speed links, facilitating distributed training. PyTorch (Paszke et al. 2019), a widely adopted deep learning framework, is compatible with the Ascend NPU through the Ascend extension for PyTorch (Zhu et al. 2023). AscendSpeed, an acceleration library tailored for Ascend devices, focuses on parallel strategy partitioning for LLMs and aggregates results through collective communication. ModelLink, a training framework designed for LLMs, fully considers the characteristics of the Ascend NPU and implements features such as memory optimization, multi-dimensional parallelism, and adaptive data loading, further enhancing training performance.

Method

In this section, we present the definition of affinity score with a rigorous formulation of expert-token affinity metrics and the implementation of our affinity-driven active selection routing. To reduce the lower bound of expert capacity, we introduce a training strategy for dynamic token distribution evolution under the guiding principle of affinity score.

Model Architecture.

Backbone. The MoE architecture, based on the Transformer framework, efficiently scales up model size with low computational overhead, benefiting from two primary structures: a sparse gating network for routing tokens and expert networks for processing specific token categories.

We consider the supervised classification for brevity where the training samples are $\{(\mathbf{x}^{(i)}, y_i)\}_{i=1}^N \sim \mathcal{D}$. Each training sample $\mathbf{x}^\top = (\mathbf{x}_1^\top, \dots, \mathbf{x}_s^\top) \in \mathcal{R}^{sd}$ has s tokens with token feature $\mathbf{x}_i \in \mathcal{R}^d, \forall i \in [s]$, and label $y \in \mathcal{N}^+$. The objective is to learn the map of \mathbf{x} to the corresponding y . The general MoE structure are formulated as

$$\text{MoE}(\mathbf{x}) = \sum_{t=1}^s \sum_{i=1}^n G_i(\mathbf{x}_t) \cdot E_i(\mathbf{x}_t), \quad (1)$$

where n is the number of experts, $G(\mathbf{x}_t): \mathcal{R}^d \rightarrow \mathcal{R}^n$ is the gating weight vector of experts which maps the tokens of \mathbf{x}_t into the corresponding experts with weights, e.g., $G_i(\mathbf{x}) = \text{Softmax}(\mathbf{W}\mathbf{x} + \epsilon)$ where the softmax is applied to each row, and $E_i(\mathbf{x}_t): \mathcal{R}^d \rightarrow \mathcal{R}$ is the i -th expert network, see (Liu et al. 2024) for current different router methods. Generally, $n \ll s$, which saves much computation compared to the dense structure.

Expert-Token Affinity. \mathbf{W}_{aff} denotes the **expert-token affinity matrix**. With GrAP as the layer of feature extraction, the formulation of \mathbf{W}_{aff} is as followed:

$$\mathbf{W}_{\text{aff}} = \begin{pmatrix} \mathbf{w}_1 & 0 & \dots & 0 \\ 0 & \mathbf{w}_2 & \dots & 0 \\ \vdots & \vdots & \ddots & \vdots \\ 0 & 0 & \dots & \mathbf{w}_n \end{pmatrix} \quad (2)$$

$$\mathbf{w}_i = \frac{n}{d} \cdot \mathbf{1} \left\{ \frac{i \cdot d}{n} \leq j < (i+1) \frac{d}{n} \right\} \quad 0 \leq j < d \quad (3)$$

The expert-token affinity matrix is employed as the gating weight to calculate the affinity score between each expert and token. We define the affinity score of t -th token and i -th expert as the cosine similarity between vectors \mathbf{x}_t and \mathbf{w}_i :

$$\delta_{ti} = \cos(\mathbf{x}_t, \mathbf{w}_i) := \mathbf{x}_t^\top \mathbf{w}_i / (\|\mathbf{x}_t\| \cdot \|\mathbf{w}_i\|) \quad (4)$$

The affinity score intuitively reflect how closely the two inputs are associated. From a perspective of semantic, the affinity scores derived from affinity metrics consisting of orthogonal vectors represent the degree of association between each token and various experts, as shown in Figure 1. Therefore, we leverage the affinity score as the principle of our affinity-driven active selection routing mechanism.

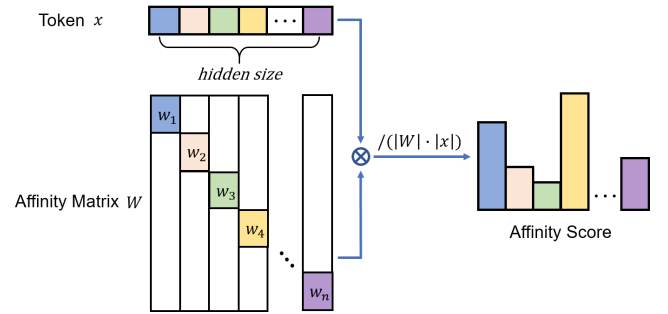


Figure 1: The illustration of affinity score.

Routing Strategy. We consider our affinity-driven active selection routing as a hybrid of TCR (Clark et al. 2022; Zhou et al. 2022) and ECR. As the name suggested, TCR lets each token choose its *top-scored* experts, and ECR lets each expert choose its *top-scored* tokens. Specifically, we use the result of the expert-token affinity metrics as the affinity score between tokens and experts. In conventional TCR routing strategy, the tokens are simply route to their Top-1 expert. In our hybrid **TCR+ECR** routing strategy, experts also select tokens for processing from assigned tokens according to affinity scores:

$$\left(\tilde{E}_{t1}, \dots, \tilde{E}_{t\ell} \right) = \text{Top-}\ell \left(\{ \delta_{t1}, \dots, \delta_{tn} \} \right), \quad (5)$$

$$\tilde{I}_{tk} \in [n], \forall t \in [s], k \in [\ell].$$

and then the expert to choose its Top- ℓ tokens where ℓ is determined by a threshold of the sum of affinity scores:

$$\left(I_{1i}, \dots, I_{Ci} \right) = \text{Bottom-}C \left(\left\{ t \in [s] : \exists j \in [\ell], \tilde{I}_{tj} = i \right\} \right),$$

$$I_{ki} \in [s] \cup \text{None}, \forall i \in [n], k \in [C]. \quad (6)$$

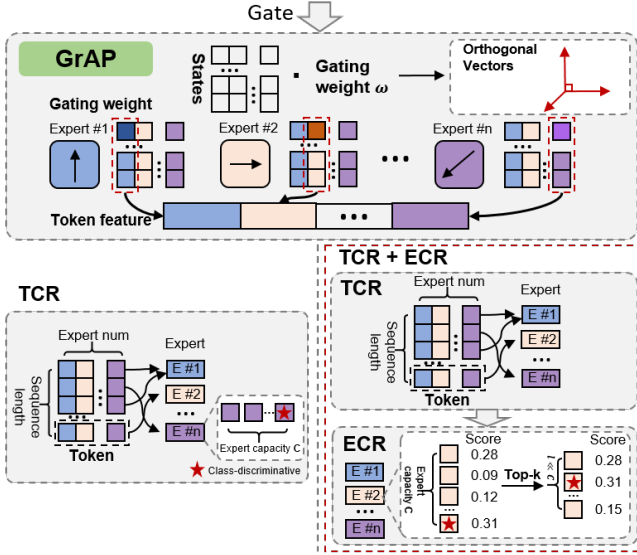


Figure 2: The architecture of the gate network along with the hybrid TCR + ECR router.

Such bidirectional selection mechanism motivates each expert to receive a certain number of tokens with the highest affinity score to itself, thereby achieving a resonance effect. The resonance effect can help mitigate the homogenization in MoE.

Locality Loss. Feed-forward network (FFN) layers are commonly employed in expert networks, allowing each expert to learn independently as a separate neural network, thus preventing interference between samples. This mechanism leads to a severe load imbalance, as experts frequently selected in the early stages are more likely to be chosen in later stages. To mitigate this skewness in token allocation, the auxiliary loss (Shazeer et al. 2017) has been proposed. Building upon the auxiliary loss, LocMoE introduces a loss bias term based on data locality, represented as $L_{\text{loc}} = \mu \text{KL}(D_c || D_1) = -\mu \int D_c(x) \ln \left[\frac{D_1(x)}{D_c(x)} \right] dx$, i.e., the Kullback-Leibler (KL) divergence of the current distribution $D_c(x)$ and the fully localized distribution $D_1(x)$. This loss term serves as a soft constraint, encouraging tokens to be sent to experts residing on the same node, thereby mitigating the substantial overhead incurred by partial inter-node communication.

Training Strategy

The Dynamic Token Distribution Evolution. Under the premises of orthogonal gating weights and a data distribution approaching uniformity, LocMoE demonstrates that the expert capacity is closely related to the angle between the gating weights and tokens. For large scale of the activation, the lower bound of expert capacity is proven to exist and is represented as $C_{\min} = \frac{1}{n} \exp\{d\delta_{\max}^2 / (2 - \delta_{\max}^2)\}$.

The hybrid TCR+ECR bidirectional selection routing, introduced in the model structure, is exemplified in the figure. If the feature fragment corresponding to the k -th dimension

of the gating weight for a particular token is more prominent, then that token will be routed to the k -th expert. If among all tokens routed to the k -th expert, there is a certain probability of the presence of class-discriminative tokens, then the capacity C must be set to a larger value to ensure the inclusion of sufficient class-discriminative tokens. The router proposed in this paper is a hybrid of TCR and ECR modes. After determining the expert to which a token will be routed, scores are calculated for the tokens assigned to each expert, and a Top- ℓ selection is performed, where ℓ^* is determined by a threshold of the sum of scores. Subsequent theoretical analysis will demonstrate the effectiveness of this hybrid routing scheme.

Theoretical Explanation To explain the motivation of our method, we show some theoretical insights in this section. Our theoretical analysis is built on Chowdhury et al. (2023), where they make the following data assumption:

Assumption 1 (data assumption). *Each input $x \in \mathcal{R}^{sd}$ with s tokens is comprised of one class-discriminative pattern $\mathbf{o}_1, \dots, \mathbf{o}_n \in \mathcal{R}^d$, with each decides the label in $[n]$, and $s - 1$ class-irrelevant patterns $\mathbf{r} \sim \mathcal{N}$ for certain distribution \mathcal{N} . For example, $x = (\mathbf{r}_1, \mathbf{r}_2, \mathbf{o}_1, \mathbf{r}_3, \dots, \mathbf{r}_{s-1})$ has label 1, where $\mathbf{r}_i \stackrel{i.i.d.}{\sim} \mathcal{N}, \forall i \in [s - 1]$.*

Based on Assumption 1, Chowdhury et al. (2023) demonstrated that the training of MoE go through two phases:

Phase 1: Router training (Chowdhury et al. 2023, Lemma 4.1 and Assumption 4.4), which makes class-discriminative patterns all to the corresponding expert. This process ensures that each expert only receives the class-discriminative tokens related to the specific class.

Phase 2: Expert training (Chowdhury et al. 2023, Theorem 4.2 and Theorem 4.5), which makes each expert learn to predict the label based on its class-discriminative inputs from Phase 1. This process is designed to establish each expert’s ability to handle and solve problems.

Hence, the training of an input in the current step is valid if the class-discriminative patterns is correctly dispatched. To quantitatively measure the difference between TCR and ECR, we define **training success rate** of input motivated by the training process of MoE.

Definition 2 (training success rate). *We say the input $x \in \mathcal{R}^{sd}$ with s tokens succeed in training if the class-discriminative pattern in x , e.g., \mathbf{o}_i is correctly dispatched to i -th expert. We further define **training success rate** as the probability that the input succeed in training.*

Furthermore, to show the quantitative comparison of TCR and ECR in training success rate, we need following assumptions and notations of token patterns.

Assumption 3 (class-discriminative). *We assume the location and feature of class-discriminative pattern is uniformly distribute in $[s]$ and $[n]$, i.e.,*

$$i \sim \text{Unif}([s]), \mathbf{x}_i \sim \text{Unif}(\{\mathbf{o}_1, \dots, \mathbf{o}_n\}).$$

We also assume that $\forall i \in [n], \mathbf{o}_i$ should be sent to the i -th expert, and define the true positive probability in token

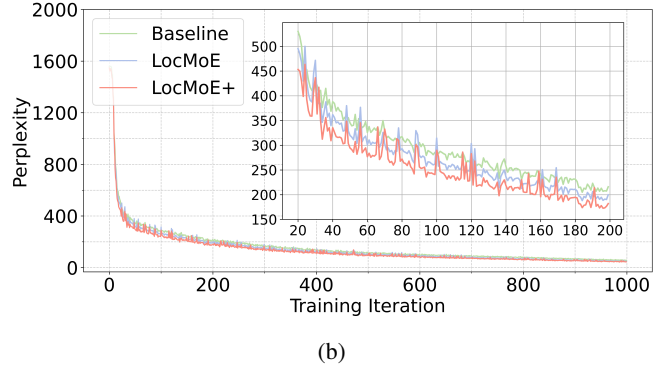
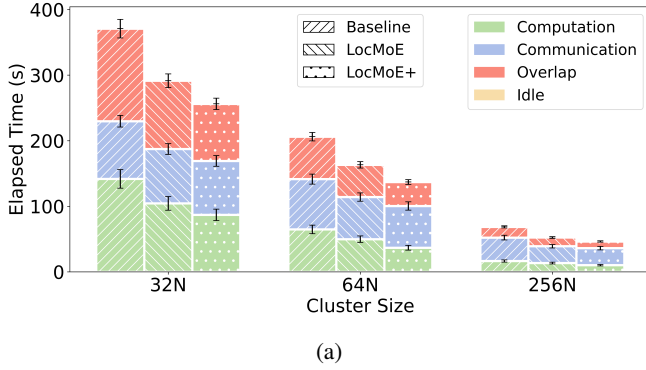


Figure 3: (a) The average composition of computation, communication, overlap, and idle with different schemes and cluster sizes. (b) The perplexity during training iterations with different schemes.

choice setting is no worse than the uniform dispatch as below

$$\mathcal{P}(\delta_{\mathbf{o}_i, i} \geq \delta_{\mathbf{x}_j, i}, \forall j \in [s]) = p_i \geq 1/n, \forall i \in [n].$$

Assumption 4 (class-irrelevant). *The distribution of class-irrelevant patterns is isotropy, i.e.,*

$$\mathcal{P}(\mathbf{r} \sim \mathcal{N}, \delta_{\mathbf{r}, i} \geq \delta_{\mathbf{x}_j, i}, \forall j \in [s]) = 1/n, \forall i \in [n]. \quad (7)$$

And we define the false positive probability in expert choice setting as

$$\mathcal{P}(\mathbf{r} \sim \mathcal{N}, \delta_{\mathbf{r}, i} \geq \delta_{\mathbf{o}_i, i}) = q_i, \forall i \in [n], \quad (8)$$

which measures the possibility that expert i chooses the wrong token \mathbf{r} instead of the correct token \mathbf{o}_i .

Assumption 3 assumes the valid token is uniformly distributed in training samples due to the massive amounts of data nowadays. Assumption 4 assumes the invalid tokens can be uniformly dispatched to experts since the invalid tokens do not provide supervised signal to router and experts in training. We consider such uniform settings are common assumptions in theoretical analysis. Now we compute the training success rate of TCR and ECR.

Theorem 5. *Under Assumptions 3 and 4, the training success rate of TCR in each sample \mathbf{x} is*

$$\mathcal{P}(\text{TCR succeed}) = \Theta\left(C \sum_{i=1}^n p_i/s\right), \quad (9)$$

and the training success rate of ECR is $\forall i \in [n]$,

$$\mathcal{P}(\text{ECR succeed}) \begin{cases} \leq \frac{1}{n} \sum_{i=1}^n e^{-\frac{(s-1)q_i}{s}}, & C \leq (s-1)q_i/2, \\ \geq 1 - e^{-3C/16}, & C \geq 2sq_i. \end{cases} \quad (10)$$

Corollary 6. *In practice, For constant number of experts (Jiang et al. 2024a), i.e., $n = \Theta(1)$, and $C < s$ to save computation cost. We have the following lower bound for capacity C to ensure high training success rate:*

1. *Suppose $q_i = \Theta(1)$. Then TCR is much better than ECR, and we only need $C = \Theta(s)$.*

2. *Suppose $\forall i \in [n], sq_i \leq C^*$ for some $C^* > 0$. Then ECR is much better than TCR, and we only need $C \geq 2C^*$.*

Remark 7. *We explain the benefit of switching TCR to ECR during training based on Theorem 5 and feature distribution during training.*

At the beginning of training, the model seldom learn the task. Then the feature of class-irrelevant tokens is nearly isotropy, e.g., uniformly distribute around the sphere (see Appendix), leading to $q_i = \Theta(1)$. The success rate of TCR with the form C/s is better than ECR with the form e^{-s} . Thus we should choose TCR with a large capacity $C = \Theta(s)$ to improve the success rate of training samples.

After training for some iterations, the experts can roughly distinguish the class-irrelevant and discriminative patterns, leading to $q_i \ll 1$ or $sq_i \leq C^*$ for some $C^* > 0$ (see Appendix). Then ECR with success rate nearly 1 is better than TCR with the form C/s as long as $C \geq 2C^*$. Thus we should choose ECR with a small capacity $C = \Theta(1)$ to improve the success rate of training samples.

Indeed, we find that Chowdhury et al. (2023, the definition of ℓ^*) consider the ECR setting and verify the benefit in sample complexity. They assume the maximum number of class-irrelevant patches that are close to class-discriminative patches are bounded, which has similar effect as C^* in our scene.

Communication Optimization

The training framework employs the Communication Over Computation (CoC) optimization technique to address performance bottlenecks in LLM training. During forward propagation in LLMs, the ColumnParallelLinear and RowParallelLinear components involve sequentially dependent computation (matrix multiplication) and communication (collective operations like AllReduce, AllGather, and ReduceScatter). These dependencies lead to inefficient serial execution. CoC decomposes these tasks into finer-grained subtasks and merges computation and communication into single kernels, such as MATMUL_ALL_REDUCE and MATMUL_REDUCE_SCATTER, utilizing MTE's remote memory access capabilities. This approach allows for pipeline-style parallel execution and overlapping of compu-

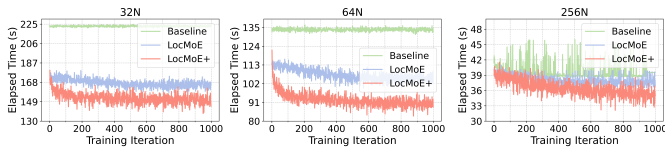


Figure 4: The time consumption during training iterations with different schemes and cluster sizes.

tation and communication, significantly enhancing overall efficiency.

Experiments

Experimental Setup

This study employs the Mixtral 8×7B model, incorporating LocMoE and our proposed approach. The Mixtral model, comprising 46.7 billion parameters and utilizing Group Query Attention (GQA), features 32 sparse expert blocks with 8 experts in the MoE Feedforward layer, where each token engages the top 2 experts for processing. Given the prevalence of long-text corpora in our application scenarios, we extended the sequence length to 32,768 and implemented tailored parallel strategies for cluster scales of 32N, 64N, and 256N, encompassing tensor, pipeline, data, and expert parallelism, with a consistent global batch size of 128. Other details of experimental setup including datasets, environment, configuration, and metrics, can be seen in Appendix.

Efficiency Promotion and Memory Footprint Reduction

As detailed in Section **Method**, we consistently use Top-1 routing to ensure the routing implementation aligns with our theoretical framework. The Baseline model utilizes a limited expert capacity mode instead of the *groupedGEMM* scheme, which avoids token dropping, with the capacity factor set to 1.1. LocMoE considers data distribution uniformity and estimates expert capacity using a lower bound formula derived from its theoretical conclusions in the first batch, maintaining it as a constant during subsequent training. Our approach (abbreviate to "LocMoE+" in figures) fixes the range of score sums, processes hidden states, and calculates current expert capacity. The subsequent analysis addresses the training time, convergence, and memory usage efficiency of these schemes on multiple sizes of Ascend clusters.

Figure 3a illustrates the time consumption of these methods during the first 1000 iterations of training. Due to initialization and some unstable factors, time consumption is recorded starting from the 5th iteration. The Baseline model's time consumption is relatively stable. As iterations increase, LocMoE's time consumption slightly decreases, particularly in 32N and 64N, consistent with the conclusion that locality loss is effective only when the number of experts is greater than or equal to the number of nodes. Our approach incurs slightly higher time consumption than LocMoE due to the computational overhead of token rearrangement. However, as token features converge, the required to-

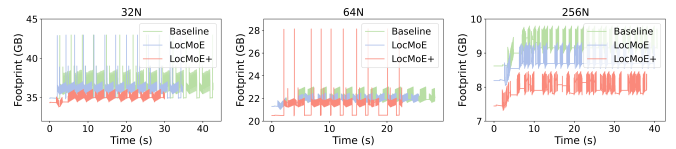


Figure 5: print recorded in one acquisition cycle with different schemes and cluster sizes.

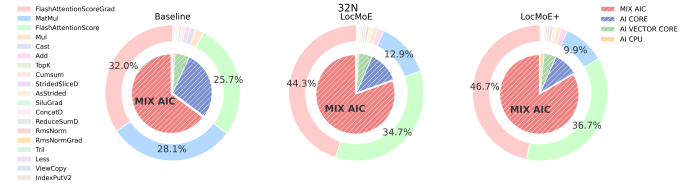


Figure 6: The distribution of time consumption for operators.

kens gradually decrease and stabilize, leading to a decline in time consumption, which remains stable in subsequent training processes. Overall, our approach reduces training time by 2.9% to 13.3% compared to LocMoE, and by 5.4% to 46.6% compared to the Baseline.

We select 10 iterations at equal intervals from the training iterations to collect data on the time consumption of computation, communication, overlap, and idle periods, as shown in Figure 3a. It is important to note that the data collection operation also introduces some overhead. After integrating LocMoE and our approach, the time consumption of each component decreases, with a significantly greater reduction in computation overhead compared to communication overhead. Additionally, as the cluster size increases, the proportion of computation/communication overlap decreases, and the magnitude of the reduction in computation overhead diminishes. Figure 3b illustrates perplexity as a measure of convergence. The convergence curves of these approaches indicate normal loss convergence, with our approach not adversely impacting convergence.

The proportional time consumption at the operator level is depicted in Figure 6. Among the components, AI CORE efficiently executes matrix multiplications and convolutions in AI algorithms; AI VECTOR CORE accelerates vector operations through parallel processing; MIX AIC integrates different types of operators and optimizes for multiple tasks; AI CPU is optimized in hardware and instruction sets to better support AI algorithms. Our approach selects fewer tokens, resulting in a 17× performance improvement in the FFN *MatMul* operator compared to the Baseline and a 2.6× improvement compared to LocMoE. This leads to an overall 2.8× reduction in the cumulative time consumption of the *MatMul* operator and a 2.6× decrease in Cube computing load. However, the proportions of *TopK* and *IndexPutV2*, related to rearrangement, show a slight increase.

We select a single iteration during the stable training period and describe the per-device memory usage (Allocated) using the first 100,000 samples from its memory monitoring, as shown in Figure 5. Overall, our approach achieves

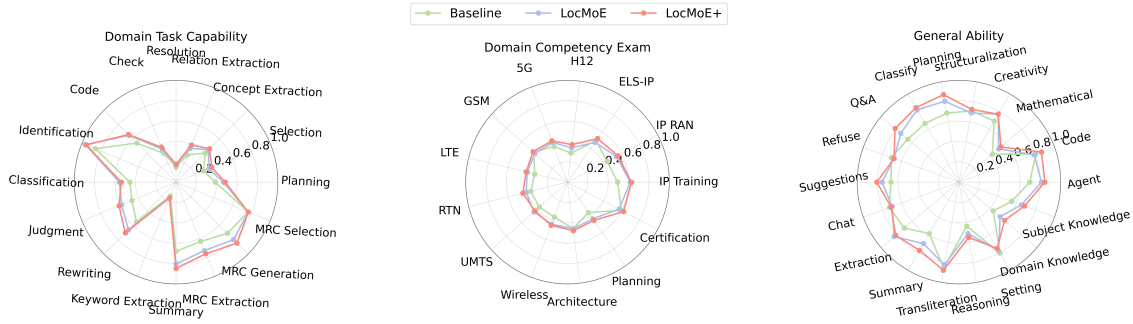


Figure 7: The performance on three categories of GDAD.

memory usage reduction of 4.57% to 16.27% compared to the Baseline and 2.86% to 10.5% compared to LocMoE. As cluster size increases, the proportion of computational overhead decreases, and the gap in memory usage narrows. Additionally, instantaneous memory peaks gradually disappear, and the fluctuation amplitude of short-term memory also diminishes.

The Performance of Downstream Tasks

To enhance the model’s conversational capabilities and adaptability to downstream task, we fine-tuned the pre-trained models. As shown in Figure 7, with sufficient supervised fine-tuning (SFT), our approach achieves an average improvement of approximately 20.1% in 16 sub-capabilities of *Domain Task Capability*, which is a portion of General and Domain-specific Assessment Dataset (GDAD), compared to the Baseline, and an increase of about 3.5% compared to LocMoE. The *Rewriting* and *Summary* capabilities show the highest improvement, with a 28.2% increase compared to the Baseline and a 6.7% increase compared to LocMoE. In the 13 tests of *Domain Competency Exam*, our approach demonstrates an average improvement of 16% relative to the Baseline and an average increase of approximately 4.8% compared to LocMoE. The *IP Training* in the digital communications domain shows the most significant improvement, with a 27.3% increase compared to the Baseline and a 3.0% increase compared to LocMoE. Among the 18 sub-capabilities of *General Ability*, our approach exhibits an improvement of about 13.9% relative to the Baseline and an average increase of 4.8% compared to LocMoE. The capability of *Planning* demonstrates the highest improvement, with a 26.8% increase compared to the Baseline and a 2.92% increase compared to LocMoE.

Table 1 presents the holistic evaluation results for multiple datasets, where GDAD-1 represents *Domain Task Capability*, and the other metrics follow accordingly. Notably, due to the 6:4 ratio of Chinese to English data in our incremental pre-training domain data and the 7:3 ratio in the fine-tuning data, our approach achieves an improvement of approximately 10.7% compared to the Baseline and 1.2% compared to LocMoE in the C-Eval (Huang et al. 2024) evaluation, despite the limited data available for training. During incremental training and fine-tuning, we incorporated substantial telecommunications domain knowledge, questions, and

Table 1: Performance promotion obtained by our approach on different datasets.

	GDAD				C-Eval	TeleQnA
	GDAD-1	GDAD-2	GDAD-3	Avg		
Baseline	47.8	43.0	65.4	52.8	38.5	62.1
LocMoE	55.5	47.6	71.1	59.0	42.6	67.6
LocMoE+	57.4	49.9	74.5	61.5	43.1	68.8

case studies. TeleQnA (Maatouk et al. 2023), the first benchmark dataset designed to evaluate the knowledge of LLMs in telecommunications, effectively measures the model’s capabilities in this domain. Consequently, our approach comprehensively surpasses both the Baseline and LocMoE on this specific dataset.

Conclusion

In this paper, we propose a novel MoE structure incorporating token feature awareness mechanism to enhance the training efficiency and performance of LLMs. Building upon the feature extraction component and locality loss of LocMoE, our approach introduces a routing strategy that combines TCR and ECR, theoretically demonstrating improved training success rates. By defining the affinity between tokens and experts, expert capacity can be dynamically reduced and further minimized. Model training experiments are conducted on Ascend clusters, leveraging the communication optimization characteristics of CoC. Our approach achieves performance improvements up to 46.6% (32N) compared to the Baseline and 13.3% (32N) compared to LocMoE, while reducing memory usage by up to 16.27% and 10.5%, respectively. To evaluate model performance, all pre-trained models are fine-tuned using a mixture of domain-specific and general data, and assessed with the open-source datasets C-Eval and TeleQnA, and closed domain benchmark GDAD. In downstream tasks, our approach outperforms the Baseline by 14.1%, 10.7%, and 9.7% on GDAD, C-Eval, and TeleQnA, respectively; it exceeds LocMoE by 4.1%, 1.2%, and 1.7% on these datasets, respectively. Both theoretical proofs and experimental results demonstrate the benefits of the proposed routing strategy for LLM training efficiency. Future work may explore methods to compress communication data to further reduce communication overhead.

References

- Achiam, J.; Adler, S.; Agarwal, S.; Ahmad, L.; Akkaya, I.; Aleman, F. L.; Almeida, D.; Altenschmidt, J.; Altman, S.; Anadkat, S.; et al. 2023. Gpt-4 technical report. *arXiv preprint arXiv:2303.08774*.
- Anil, R.; Dai, A. M.; Firat, O.; Johnson, M.; Lepikhin, D.; Passos, A.; Shakeri, S.; Taropa, E.; Bailey, P.; Chen, Z.; et al. 2023. Palm 2 technical report. *arXiv preprint arXiv:2305.10403*.
- Bajaj, P.; Xiong, C.; Ke, G.; Liu, X.; He, D.; Tiwary, S.; Liu, T.-Y.; Bennett, P.; Song, X.; and Gao, J. 2022. Metro: Efficient denoising pretraining of large scale autoencoding language models with model generated signals. *arXiv preprint arXiv:2204.06644*.
- Cao, Z.; Sun, Q.; Yang, W.; Song, C.; Wang, Z.; and Li, H. 2024. A novel HPL-AI approach for FP16-only accelerator and its instantiation on Kunpeng+ Ascend AI-specific platform. *Journal of Parallel and Distributed Computing*, 190: 104884.
- Chowdhury, M. N. R.; Zhang, S.; Wang, M.; Liu, S.; and Chen, P.-Y. 2023. Patch-level routing in mixture-of-experts is provably sample-efficient for convolutional neural networks. In *International Conference on Machine Learning*, 6074–6114. PMLR.
- Chung, F.; and Lu, L. 2006. Concentration inequalities and martingale inequalities: a survey. *Internet mathematics*, 3(1): 79–127.
- Clark, A.; de Las Casas, D.; Guy, A.; Mensch, A.; Paganini, M.; Hoffmann, J.; Damoc, B.; Hechtman, B.; Cai, T.; Borgeaud, S.; et al. 2022. Unified scaling laws for routed language models. In *International conference on machine learning*, 4057–4086. PMLR.
- Dai, D.; Deng, C.; Zhao, C.; Xu, R.; Gao, H.; Chen, D.; Li, J.; Zeng, W.; Yu, X.; Wu, Y.; et al. 2024. Deepseekmoe: Towards ultimate expert specialization in mixture-of-experts language models. *arXiv preprint arXiv:2401.06066*.
- Dai, D.; Dong, L.; Ma, S.; Zheng, B.; Sui, Z.; Chang, B.; and Wei, F. 2022. Stablemoe: Stable routing strategy for mixture of experts. *arXiv preprint arXiv:2204.08396*.
- Du, N.; Huang, Y.; Dai, A. M.; Tong, S.; Lepikhin, D.; Xu, Y.; Krikun, M.; Zhou, Y.; Yu, A. W.; Firat, O.; et al. 2022. Glam: Efficient scaling of language models with mixture-of-experts. In *International Conference on Machine Learning*, 5547–5569. PMLR.
- Fedus, W.; Zoph, B.; and Shazeer, N. 2022. Switch transformers: Scaling to trillion parameter models with simple and efficient sparsity. *Journal of Machine Learning Research*, 23(120): 1–39.
- Floridi, L.; and Chiriatti, M. 2020. GPT-3: Its nature, scope, limits, and consequences. *Minds and Machines: Journal for Artificial Intelligence, Philosophy and Cognitive Science*.
- Guo, Y.; Cheng, Z.; Tang, X.; and Lin, T. 2024. Dynamic Mixture of Experts: An Auto-Tuning Approach for Efficient Transformer Models. *arXiv preprint arXiv:2405.14297*.
- Hazimeh, H.; Zhao, Z.; Chowdhery, A.; Sathiamoorthy, M.; Chen, Y.; Mazumder, R.; Hong, L.; and Chi, E. 2021. Dselect-k: Differentiable selection in the mixture of experts with applications to multi-task learning. *Advances in Neural Information Processing Systems*, 34: 29335–29347.
- Hoffmann, J.; Borgeaud, S.; Mensch, A.; Buchatskaya, E.; Cai, T.; Rutherford, E.; Casas, D. d. L.; Hendricks, L. A.; Welbl, J.; Clark, A.; et al. 2022. Training compute-optimal large language models. *arXiv preprint arXiv:2203.15556*.
- Huang, Y.; Bai, Y.; Zhu, Z.; Zhang, J.; Zhang, J.; Su, T.; Liu, J.; Lv, C.; Zhang, Y.; Fu, Y.; et al. 2024. C-eval: A multi-level multi-discipline chinese evaluation suite for foundation models. *Advances in Neural Information Processing Systems*, 36.
- Jiang, A. Q.; Sablayrolles, A.; Roux, A.; Mensch, A.; Savary, B.; Bamford, C.; Chaplot, D. S.; Casas, D. d. l.; Hanna, E. B.; Bressand, F.; et al. 2024a. Mixtral of experts. *arXiv preprint arXiv:2401.04088*.
- Jiang, Z.; Lin, H.; Zhong, Y.; Huang, Q.; Chen, Y.; Zhang, Z.; Peng, Y.; Li, X.; Xie, C.; Nong, S.; et al. 2024b. {MegaScale}: Scaling Large Language Model Training to More Than 10,000 {GPUs}. In *21st USENIX Symposium on Networked Systems Design and Implementation (NSDI 24)*, 745–760.
- Kenton, J. D. M.-W. C.; and Toutanova, L. K. 2019. BERT: Pre-training of Deep Bidirectional Transformers for Language Understanding. In *Proceedings of NAACL-HLT*, 4171–4186.
- Lepikhin, D.; Lee, H.; Xu, Y.; Chen, D.; Firat, O.; Huang, Y.; Krikun, M.; Shazeer, N.; and Chen, Z. 2020. GShard: Scaling Giant Models with Conditional Computation and Automatic Sharding. In *International Conference on Learning Representations*.
- Lepikhin, D.; Lee, H.; Xu, Y.; Chen, D.; Firat, O.; Huang, Y.; Krikun, M.; Shazeer, N.; and Chen, Z. 2020. Gshard: Scaling giant models with conditional computation and automatic sharding. *arXiv preprint arXiv:2006.16668*.
- Li, J.; Jiang, Y.; Zhu, Y.; Wang, C.; and Xu, H. 2023. Accelerating distributed {MoE} training and inference with lina. In *2023 USENIX Annual Technical Conference (USENIX ATC 23)*, 945–959.
- Li, J.; Sun, Z.; He, X.; Zeng, L.; Lin, Y.; Li, E.; Zheng, B.; Zhao, R.; and Chen, X. 2024. Locmoe: A low-overhead moe for large language model training. *arXiv preprint arXiv:2401.13920*.
- Liu, T.; Blondel, M.; Riquelme, C.; and Puigcerver, J. 2024. Routers in Vision Mixture of Experts: An Empirical Study. *arXiv preprint arXiv:2401.15969*.
- Maatouk, A.; Ayed, F.; Piovesan, N.; De Domenico, A.; Debbah, M.; and Luo, Z.-Q. 2023. Teleqna: A benchmark dataset to assess large language models telecommunications knowledge. *arXiv preprint arXiv:2310.15051*.
- Paszke, A.; Gross, S.; Massa, F.; Lerer, A.; Bradbury, J.; Chanan, G.; Killeen, T.; Lin, Z.; Gimelshein, N.; Antiga, L.; et al. 2019. Pytorch: An imperative style, high-performance deep learning library. *Advances in neural information processing systems*, 32.

- Radford, A.; Narasimhan, K.; Salimans, T.; Sutskever, I.; et al. ????. Improving language understanding by generative pre-training.
- Rajbhandari, S.; Li, C.; Yao, Z.; Zhang, M.; Aminabadi, R. Y.; Awan, A. A.; Rasley, J.; and He, Y. 2022. Deepspeed-moe: Advancing mixture-of-experts inference and training to power next-generation ai scale. In *International conference on machine learning*, 18332–18346. PMLR.
- Riquelme, C.; Puigcerver, J.; Mustafa, B.; Neumann, M.; Jenatton, R.; Susano Pinto, A.; Keysers, D.; and Houlsby, N. 2021. Scaling vision with sparse mixture of experts. *Advances in Neural Information Processing Systems*, 34: 8583–8595.
- Roller, S.; Sukhbaatar, S.; Weston, J.; et al. 2021. Hash layers for large sparse models. *Advances in Neural Information Processing Systems*, 34: 17555–17566.
- Shazeer, N.; Mirhoseini, A.; Maziarz, K.; Davis, A.; Le, Q.; Hinton, G.; and Dean, J. 2017. Outrageously large neural networks: The sparsely-gated mixture-of-experts layer. *arXiv preprint arXiv:1701.06538*.
- Tang, Y.; and Wang, C.-l. 2023. Performance modeling on DaVinci AI core. *Journal of Parallel and Distributed Computing*, 175: 134–149.
- Wang, X.; Zhang, H.; and Du, Z. 2023. Multi-scale noise reduction attention network for aero-engine bearing fault diagnosis. *IEEE Transactions on Instrumentation and Measurement*.
- Wei, A.; Haghtalab, N.; and Steinhardt, J. 2024. Jailbroken: How does llm safety training fail? *Advances in Neural Information Processing Systems*, 36.
- Xia, J.; Cheng, C.; Zhou, X.; Hu, Y.; and Chun, P. 2021. Kunpeng 920: The first 7-nm chiplet-based 64-core arm soc for cloud services. *IEEE Micro*, 41(5): 67–75.
- Xie, Z.; Zhang, Y.; Zhuang, C.; Shi, Q.; Liu, Z.; Gu, J.; and Zhang, G. 2024. MoDE: A Mixture-of-Experts Model with Mutual Distillation among the Experts. In *Proceedings of the AAAI Conference on Artificial Intelligence*, volume 38, 16067–16075.
- Yang, Y.; Qi, S.; Gu, W.; Wang, C.; Gao, C.; and Xu, Z. 2024. Enhancing Efficiency in Sparse Models with Sparsers Selection. *arXiv preprint arXiv:2403.18926*.
- Zhao, W. X.; Zhou, K.; Li, J.; Tang, T.; Wang, X.; Hou, Y.; Min, Y.; Zhang, B.; Zhang, J.; Dong, Z.; et al. 2023. A survey of large language models. *arXiv preprint arXiv:2303.18223*.
- Zhou, Y.; Du, N.; Huang, Y.; Peng, D.; Lan, C.; Huang, D.; Shakeri, S.; So, D.; Dai, A. M.; Lu, Y.; et al. 2023. Brainformers: Trading simplicity for efficiency. In *International Conference on Machine Learning*, 42531–42542. PMLR.
- Zhou, Y.; Lei, T.; Liu, H.; Du, N.; Huang, Y.; Zhao, V.; Dai, A. M.; Le, Q. V.; Laudon, J.; et al. 2022. Mixture-of-experts with expert choice routing. *Advances in Neural Information Processing Systems*, 35: 7103–7114.
- Zhu, Z.; Wang, B.; Yang, C.; Zhu, R.; Zhou, M.; and Zheng, N. 2023. Performance Evaluation of MindSpore and PyTorch Based on Ascend NPU. In *2023 IEEE 29th International Conference on Parallel and Distributed Systems (ICPADS)*, 1826–1832. IEEE.

Appendix

Missing Proof

Auxiliary Results

Lemma 8 (Theorem 4 in (Chung and Lu 2006)). *Let $\mathbf{X}_1, \dots, \mathbf{X}_n$ be n independent random variables with*

$$\mathcal{P}(\mathbf{X}_i = 1) = p_i, \mathcal{P}(\mathbf{X}_i = 0) = 1 - p_i.$$

We consider the sum $\mathbf{X} = \sum_{i=1}^n \mathbf{X}_i$, with expectation $\mathcal{E}(\mathbf{X}) = \sum_{i=1}^n p_i$. Then we have

$$\begin{aligned} \text{(Lower tail)} \quad \mathcal{P}(\mathbf{X} \leq \mathcal{E}\mathbf{X} - \lambda) &\leq e^{-\frac{\lambda^2}{2\mathcal{E}\mathbf{X}}}, \\ \text{(Upper tail)} \quad \mathcal{P}(\mathbf{X} \geq \mathcal{E}\mathbf{X} + \lambda) &\leq e^{-\frac{\lambda^2}{2(\mathcal{E}\mathbf{X} + \lambda/3)}}. \end{aligned} \quad (11)$$

Proof of Theorem 5

Proof. 1) For the TCR, denote

$$s_i = |\{t < k : \mathbf{x}_t \text{ sent to expert } i, \mathbf{x}_k = \mathbf{o}_i\}|, \forall i \in [n]$$

as the top class-irrelevant token number candidate to the i -th expert before the valid token. Then by Assumption 4, each class-irrelevant token uniformly gives to any expert, leading to $s_i | (\mathbf{x}_k = \mathbf{o}_i) \sim \mathcal{B}(k-1, 1/n)$ (Binomial distribution), i.e., $\forall t \in [k-1]$,

$$\mathcal{P}(s_i = t | \mathbf{x}_k = \mathbf{o}_i) = \binom{k-1}{t} \cdot \left(\frac{1}{n}\right)^t \left(1 - \frac{1}{n}\right)^{k-1-t}.$$

Then we could derive that

$$\begin{aligned} \mathcal{P}(\mathbf{x} \text{ succeed in training}) &= \sum_{i=1}^n \mathcal{P}(\mathbf{o}_i \text{ sent to expert } i | \mathbf{o}_i \text{ is in } \mathbf{x}) \cdot \mathcal{P}(\mathbf{o}_i \text{ is in } \mathbf{x}) \\ &= \frac{1}{ns} \sum_{i=1}^n \sum_{k=1}^s p_i \mathcal{P}(s_i < C | \mathbf{x}_k = \mathbf{o}_i) \\ &= \frac{1}{ns} \sum_{i=1}^n p_i \left(C + \sum_{k=C+1}^s \mathcal{P}(s_i < C | \mathbf{x}_k = \mathbf{o}_i) \right). \end{aligned} \quad (12)$$

Note that $\mathcal{E}s_i = (k-1)/n$. When $k \geq 2nC$, by lower tail bound in Lemma 8, we get

$$\mathcal{P}(s_i < C | \mathbf{x}_k = \mathbf{o}_i) \leq e^{-\frac{(k-1-n(C-1))^2}{2(k-1)n}} \leq e^{-\frac{k-1}{8n}}.$$

Hence, we get the upper bound that

$$\begin{aligned} \mathcal{P}(\mathbf{x} \text{ succeed in training}) &\stackrel{(12)}{\leq} \frac{1}{ns} \sum_{i=1}^n \sum_{k=1}^s p_i \mathcal{P}(s_i < C | \mathbf{x}_k = \mathbf{o}_i) \\ &= \frac{1}{ns} \sum_{i=1}^n p_i \left(2nC + \sum_{k=2nC+1}^s \mathcal{P}(s_i < C | \mathbf{x}_k = \mathbf{o}_i) \right) \\ &\leq \frac{1}{ns} \sum_{i=1}^n p_i \left(2nC + \sum_{k=2nC}^{s-1} e^{-\frac{k}{8n}} \right) \\ &\leq \frac{1}{ns} \sum_{i=1}^n p_i \left(2nC + \frac{e^{-\frac{C}{4}}}{1 - e^{-\frac{1}{8n}}} \right) \\ &\stackrel{(i)}{\leq} \frac{1}{ns} \sum_{i=1}^n p_i \left(2nC + (8n+1)e^{-\frac{C}{4}} \right) \leq \frac{10C \sum_{i=1}^n p_i}{s}, \end{aligned}$$

where (i) uses the inequality that $e^{-t} \leq 1/(1+t), \forall t \geq 0$.

Moreover, for $1 + \frac{nC}{4} \leq k \leq 1 + \frac{nC}{2}$, i.e., $2(k-1) \leq nC \leq 4(k-1)$, by upper tail bound in Lemma 8, we get

$$\begin{aligned} \mathcal{P}(s_i < C | \mathbf{x}_k = \mathbf{o}_i) &= 1 - \mathcal{P}(s_i \geq C | \mathbf{x}_k = \mathbf{o}_i) \\ &\geq 1 - e^{-\frac{3(nC-k+1)^2}{2n[2(k-1)+nC]}} \geq 1 - e^{-\frac{k-1}{4n}}. \end{aligned}$$

Hence, we get the lower bound that

$$\begin{aligned} \mathcal{P}(\mathbf{x} \text{ succeed in training}) &\stackrel{(12)}{\geq} \frac{1}{ns} \sum_{i=1}^n \sum_{k=1}^s p_i \mathcal{P}(s_i < C | \mathbf{x}_k = \mathbf{o}_i) \\ &= \frac{1}{ns} \sum_{i=1}^n p_i \left(\sum_{k=\lceil 1+nC/4 \rceil}^{\lfloor 1+nC/2 \rfloor} \mathcal{P}(s_i < C | \mathbf{x}_k = \mathbf{o}_i) \right) \\ &\geq \frac{1}{ns} \sum_{i=1}^n p_i \left(\frac{nC}{4} - 1 - \sum_{k=\lceil 1+nC/4 \rceil}^{\lfloor 1+nC/2 \rfloor} e^{-\frac{k-1}{4n}} \right) \\ &\geq \frac{1}{ns} \sum_{i=1}^n p_i \left(\frac{nC}{4} - 1 - \frac{e^{-\frac{C}{16}}}{1 - e^{-\frac{1}{4n}}} \right) \\ &\stackrel{(i)}{\geq} \frac{1}{ns} \sum_{i=1}^n p_i \left(\frac{nC}{4} - 2 - (4n+1)e^{-\frac{C}{16}} \right) \geq \frac{C \sum_{i=1}^n p_i}{5s}, \end{aligned}$$

where (i) uses the inequality that $e^{-t} \leq 1/(1+t), \forall t \geq 0$, and the final inequality needs $C \geq 48$, which can be satisfied in common experiments. Combining the upper and lower bounds, we obtain the desired result.

2) For the ECR, denote s_i as the class-irrelevant token number with the score larger than \mathbf{o}_i for i -th expert. By Assumption 4, we derive that $s_i \sim \mathcal{B}(s-1, q_i), \forall i \in [n]$.

$\mathcal{P}(\mathbf{x} \text{ succeed in training})$

$$\begin{aligned} &= \sum_{i=1}^n \mathcal{P}(\text{expert } i \text{ choose } \mathbf{o}_i | \mathbf{o}_i \text{ is in } \mathbf{x}) \mathcal{P}(\mathbf{o}_i \text{ is in } \mathbf{x}) \\ &= \frac{1}{n} \sum_{i=1}^n \mathcal{P}(s_i \leq C-1, s_i \sim \mathcal{B}(s-1, q_i)) \end{aligned}$$

If $C-1 \leq (s-1)q_i/2$, by lower tail bound in Lemma 8 with $\lambda = (s-1)q_i - (C-1) < \mathcal{E}s_i$, we obtain that

$$\mathcal{P}(s_i \leq C-1) \leq e^{-\frac{(s-1)q_i}{2} \left(1 - \frac{C-1}{(s-1)q_i}\right)^2} \leq e^{-\frac{(s-1)q_i}{8}}.$$

If $C \geq 2(s-1)q_i$, by upper tail bound in Lemma 8 with $\lambda = C - (s-1)q_i > 0$, we obtain that

$$\begin{aligned} \mathcal{P}(s_i \leq C-1) &= 1 - \mathcal{P}(s_i \geq C) \\ &\geq 1 - e^{-\frac{[C-(s-1)q_i]^2}{2(C+2(s-1)q_i)/3}} \geq 1 - e^{-\frac{3C}{16}}. \end{aligned}$$

Hence, we conclude Eq. (10). \square

Token Feature Distribution

We also validate the feature distribution before and after MoE training shown in Figure 8. We can see before training,

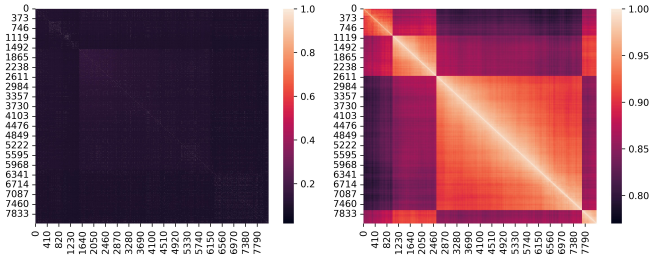


Figure 8: The correlation matrix of one training sample feature before (left) and after (right) training.

all 8192 tokens in one training sample are nearly orthogonal with correlation coefficient near zero, which verifies the isotropy distribution assumption in the first bullet of Remark 7. After training, the token features are nearly aligned with correlation coefficient large than 0.8. We can also observe that neighbouring tokens share similar features, and clear block feature behavior, meaning that the token features are relatively separated and the number of tokens in each cluster is bounded, which somehow matches the distribution assumption in the second bullet of Remark 7.

Experimental Setup

Datasets for Training and Fine-Tuning

The dataset used in this paper is a self-constructed dataset that integrates knowledge from multiple domains, including wireless, data communication, and cloud-core technologies. It comprises Chinese, English, and bilingual corpora. The corpora are parsed from various internal technical documents, such as iCase, blogs, Wiki, and feature documents. Taking iCase as an example, iCase is a case record of problem localization and handling processes, containing code, instructions, and corresponding logs. In addition, the above-mentioned domain-specific knowledge corpora are mixed with general corpora in a ratio of 1:5. The general corpora are collected from hundreds of websites, including online novels, cooking guides, movie reviews, and more. After cleaning, deduplication, and review operations, the dataset is thoroughly shuffled. A total of 4.19 billion tokens is sampled as the experimental pre-training dataset. To evaluate downstream tasks, this paper also adopt hybrid sft data items to fine-tune the pre-trained model. The dataset comprises 762,321 general question-answer pairs and 11,048 domain-specific question-answer pairs, with a general-to-domain ratio of 68:1. The general characteristics encompass multi-tasking, mathematical ability, coding ability, logical reasoning, multi-turn dialogue, knowledge reasoning, language understanding, text generation, multi-tasking, FunctionCall, CoT, MRC summarization, refusal to answer, Chinese, and English. The domain-specific characteristics include domain knowledge understanding, RAG, Function-Call, information extraction, multi-turn dialogue, reading comprehension, paraphrasing, and intent recognition.

Experimental Environment

The experiments are conducted on a cluster composed of Ascend 910B3 NPUs, divided into three groups: 32 NPUs (hereinafter referred to as 32N, and so on), 64N, and 256N. The 910B3 series NPU contains 20 AI cores with a main frequency of 1.8GHz and a theoretical computing power of 313T under fp16 precision. The physical High Bandwidth Memory (HBM) of the 910B3 NPU is 64G, with an HBM frequency of 1.6GHz and an HBM bandwidth of 1.6T. Every 8 NPUs are mounted on the same Atlas 800T A2 server, which internally adopts a fullmesh networking scheme, meaning that any two NPUs are interconnected. The version of the Ascend Hardware Development Kit (HDK) is 23.0.2.1, and the version of the Compute Architecture for Neural Networks (CANN) suite is 7.0.0, which is the commercial release version for Q4 2023. The models in this paper use ModelLink, an LLM training framework based on the Ascend architecture, and run in the torch_npu 5.0.0 environment.

Model Configuration

This paper adopts the Mixtral $8 \times 7B$ model with an MoE structure, released in December 2023, as the backbone and embeds LocMoE and our approach. Mixtral has 46.7B parameters and uses the Group Query Attention (GQA) mechanism to compute attention. It contains 32 sparse expert blocks, with the MoE Feedforward layer comprising 8 experts, and each token selects the top 2 experts for processing. In the application scenarios of this paper, the corpora are generally long texts; thus, the sequence length is adjusted to 32768. For the three cluster scales of 32N, 64N, and 256N, the parallel strategies are set as follows: 32N - tensor parallel (TP=4) / pipeline parallel (PP=4) / data parallel (DP=2) / expert parallel (EP=2), 64N - TP=8 / PP=4 / DP=2 / EP=2, and 256N - TP=8 / PP=8 / DP=4 / EP=2. The batch size is set to 128.

Evaluation Metrics and Datasets

To evaluate model performance, this paper designs a comprehensive metric called the General and Domain-specific Assessment Dataset (GDAD), which consists of three evaluation systems: domain task capability, domain capability certification exam, and general capability. Among them, the domain task capability includes a total of 16 categories and 2,657 questions, such as domain logical reasoning; the domain capability certification exam includes a total of 13 categories and 13,968 questions, such as data communication; and the general capability includes a total of 18 categories and 1,435 questions, such as programming ability. The questions include objective and subjective questions in Chinese, English, and bilingual formats. For subjective questions, the cosine similarity between the model output and the standard answer is used as the score. In addition, this paper also employs C-Eval (Huang et al. 2024) and TeleQnA (Maatouk et al. 2023) to evaluate the model's Chinese language capability.